Influence of substrate structure on cleavage by hammerhead ribozyme

Daniela Scarabino[a,*], Glauco P. Tocchini-Valentini[b,c]

[a] *EniChem SpA, Istituto Guido Donegani, Via Ramarini 32, 0016 Monterotondo/Rome, Italy*
[b] *Institute of Cell Biology, CNR, Viale Marx 43, 00137 Rome, Italy*
[c] *Department of Biochemistry and Molecular Biology, University of Chicago, Chicago, IL 60637, USA*

Received 9 February 1996

Abstract We compared the cleavage by a hammerhead ribozyme of a wild-type precursor tRNA (pre-tRNA$_3^{leu}$) and a structurally altered mutant form. We also analyzed the cleavage reactions of these tRNAs catalyzed by a ribozyme variant that was designed to complement the mutant precursor tRNA. Kinetic analyses reveal that the k_{cat} values are nearly the same for the wild-type and the mutant substrate RNAs. However, the K_m values differ considerably, being higher for the wild-type substrate. Thus, the formation of the ribozyme-substrate complex, but not the chemical cleavage step, is affected by these changes. Time course studies were performed, at different temperatures, to estimate the efficiency of the cleavage reactions and the effect of temperature. The cleavage of mutant precursor tRNA is generally faster than the wild-type at all temperatures analyzed. These results suggest that substrate structures can limit ribozyme efficiency, presumably by hindering the hybridization step.

Key words: Hammerhead ribozyme; Pre-tRNA; RNA structure; Kinetics; Thermodynamics

1. Introduction

Ribozymes are RNA molecules that can catalyze chemical reactions [1,2]; many catalyze site-specific RNAs cleavage [3–5]. Comparison of sequences near the cleavage site of several self-cleaving plant RNAs has led to the identification of a consensus secondary structure termed the 'hammerhead' [6]. Recently, the three-dimensional structure of the hammerhead has been described [7,8]. The hammerhead consists of three helices of variable length and a sequence of 11 unpaired nucleotides surrounding the cleavage site. Truncation experiments confirmed that this portion of the RNA molecule suffices for the self-cleaving activity [9,10]. Although the sequence that can form the hammerhead structure is contained within a single RNA molecule, intermolecular assembly and cleavage can be achieved by dividing the domain into ribozyme and substrate molecules that associate through base pairing [11–13]. By flanking the hammerhead motif with an antisense sequence, Haseloff and Gerlach [14] demonstrated cleavage of specific target RNAs. The only sequence requirement at the cleavage site is a trinucleotide GUC (or a limited number of other triplets). Since appropriate target trinucleotides are common in RNAs, such hammerhead ribozymes can be targeted to many positions in different RNAs. Upon cleavage of the substrate, the products can dissociate from the ribozyme, allowing turnover [11,14,15].

Such custom-designed ribozymes provide highly flexible tools to inhibit the expression of specific genes, with potential therapeutic value; they constitute an alternative to antisense constructs designed to inhibit translation [16–19]. Since ribozymes recognize specific sequences in RNA by base-pairing, the design of a therapeutic ribozyme could ultimately be much simpler than the development of new inhibitors directed at a protein's active sites. The rules for developing a ribozyme for one target can be used to develop a ribozyme for many other targets. In contrast, protein active sites are idiosyncratic.

The kinetic and structural characterization of hammerhead ribozymes [20] has two points of consideration relevant for the design of ribozymes as endonucleases directed against specific target mRNAs. First, helix length and base composition will probably determine how well a particular ribozyme will function catalytically under physiological conditions. If very stable helices are generated during the binding of the ribozyme to the target RNA, product dissociation may become rate limiting for multiple turnover. Second, the structure of the target RNA will contribute to catalytic efficiency. Sequestering of the target sequence in a stable secondary or tertiary structures that are incompatible with hammerhead domain assembly, can greatly increase the concentrations required to achieve maximum cleavage rates. At worst, stable target structures may fail to assemble into the hammerhead domain altogether and may remain completely resistant to cleavage.

To investigate these problems, we examine here the temperature dependence and kinetics of ribozyme-catalyzed cleavage reactions using a precursor tRNA from yeast (pre-tRNA$_3^{leu}$) and a mutant in which the substitution of three bases alters the tRNA structure [21].

2. Materials and methods

2.1. Preparation of RNA

Genes for the wild-type yeast pre-tRNA$_3^{leu}$ and the mutant Sm (Fig. 1), under control of the T7 promoter, were assembled from a set of 12 oligodeoxynucleotides [22], and cloned into the *Pst*I-*Bam*HI site of the vector pUC19. In these constructs, transcription by T7 RNA polymerase starts exactly at the 5′-end of the pre-tRNA$_3^{leu}$ gene and terminates at a *Bst*NI site at the 3′-end, ensuring that the transcript terminates with 5′-CCA-3′.

To synthesize tRNA precursors, plasmid DNAs were cleaved with *Bst*NI restriction enzyme and transcribed with T7 RNA polymerase [23]. In the transcription reactions the final concentration of [α-^{32}P]UTP was 100 μM. Transcripts were purified by polyacrylamide gel electrophoresis, located by autoradiography, eluted in 0.5 M sodium acetate pH 7, 1 mM EDTA, and concentrated by ethanol precipitation. RNAs were dissolved in H_2O and stored at −20°C.

Ribozymes were synthesized by T7 RNA polymerase transcription of partially duplex synthetic DNA templates [24]. A typical 150 μl reaction contained 40 mM Tris-HCl pH 8.1, 10 mM $MgCl_2$, 1 mM spermidine, 0.01% Triton X-100, 5 mM DTT, 8% ethylene glycol (8000 MW), 0.3 mM template, T7 RNA polymerase at 15 U/μl, and the four NTPs (each at 4 mM). Transcription reactions were carried out at 37°C for 3 h. The transcripts were concentrated by ethanol precipitation and purified on 20% polyacrylamide 7 M urea gels. Products were located by UV shadowing, the excised bands were

*Corresponding author. Fax: (39) (6) 90673323.

SSDI S0014-5793(96)00242-6

crushed and then soaked for 2 h in 2 vols. of 0.5 M NaOAc pH 7, 1 mM EDTA. The extracted RNA was concentrated by ethanol precipitation and resuspended in H_20.

Because most transcription reactions generate multiple products that are smaller or larger than the desired RNA, care was taken to identify the correct transcript. The RNAs were sequenced by partial enzymatic digestion.

2.2. Cleavage assays

Cleavage reactions were performed in 50 mM Tris-HCl pH 8, 10 mM $MgCl_2$ at eight different temperatures ranging from 25°C to 60°C, using a ribozyme concentration of 66 nM, and a substrate concentration of 0.2 μM. To disrupt aggregation states potentially formed during RNA storage [25], solutions of both ribozyme and substrate RNAs were heated separately in 50 mM Tris-HCl pH 8 at 90°C for 1 min and allowed to cool slowly to 25°C. Each RNA solution was than adjusted to a final concentration of 10 mM $MgCl_2$ and allowed to incubate at 25°C for 15 min. Cleavage reactions were initiated by the addition of ribozyme to the substrate and buffer. Samples of 5 μl were removed at intervals, quenched with an equal volume of stop mix (7 M urea, 50 mM EDTA, 0.05% bromophenol blue, 0.05% xylene cyanol), and then fractionated by electrophoresis into 16% polyacrylamide 7 M urea gels. Substrate and product bands were located by autoradiography excised and counted to determine the fraction of cleavage.

2.3. Determination of ribozyme steady-state parameters

Kinetic reactions were performed essentially as described by Fedor and Uhlenbeck [20]. Stock solutions of 1.3 μM ribozyme and 15 μM substrate were prepared in 50 mM Tris-HCl (pH 8), preheated separately at 90°C for 1 min, and cooled to 25°C for 15 min. After $MgCl_2$ was added to a final concentration of 10 mM, the stock solutions were incubated for another 15 min at 25°C. Cleavage reactions were performed in a 50 μl volume in the presence of 10 mM $MgCl_2$, 50 mM Tris-HCl pH 8, at 50°C with 0.025 μM ribozyme and concentrations of substrate between 0.05 and 5 μM. Reactions were initiated by the addition of ribozyme to substrate.

The cleavage reactions were analyzed by electrophoresis on 16% polyacrylamide 7 M urea gels and located by autoradiography. The bands were excised and counted. All kinetic parameters were determined from Eadie-Hofstee plots [26,27].

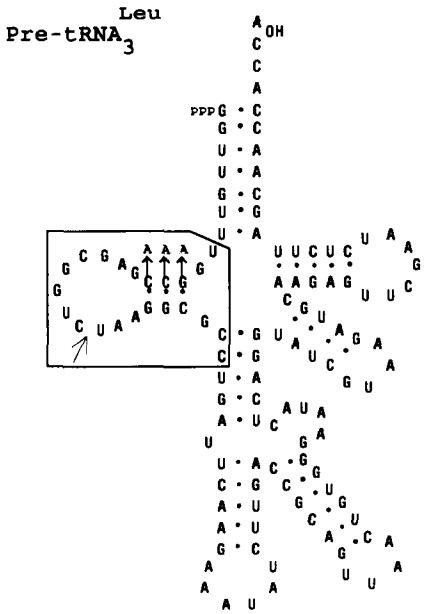

Fig. 1. Secondary structure model of pre-tRNA$_3^{leu}$ of yeast. The triple base-substitution that forms the mutant (Sm) with a disrupted D stem is indicated. The region that binds ribozymes is boxed. The cleavage site is indicated by the arrow.

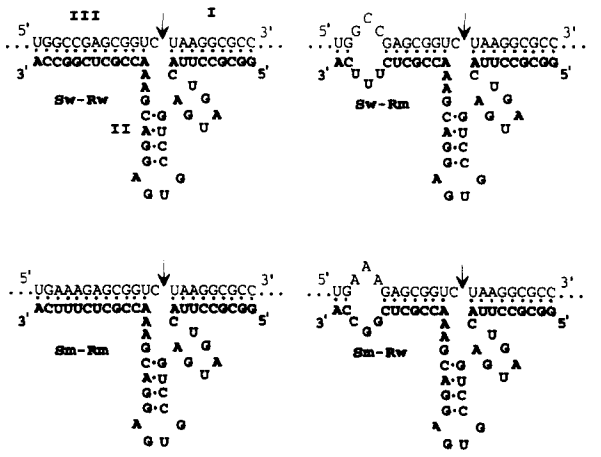

Fig. 2. Hammerhead ribozymes targeted against the pre-tRNA$_3^{leu}$ wild type and mutant. The ribozymes (bold letters) are shown complexed to their target sequences. The cleavage sites are indicated by arrows.

3. Results

3.1. Design of ribozymes

To investigate the influence of target RNA structure on the efficiency of a ribozyme catalyzed cleavage reaction, the wild-type (Sw) and the mutant form (Sm) of the pre-tRNA$_3^{leu}$ of yeast were chosen as targets (Fig. 1). In the mutant tRNA the substitution of three bases (GCC at positions 10,11,12 with AAA) prevents the formation of the D stem (Fig. 1), which is expected to further disrupt tertiary interactions in the tRNA [21]. Both tRNAs contain the potential cleavage site GUC (Fig. 1).

We designed two hammerhead ribozymes which should be able to cleave the two pre-tRNAs at the same site, one specific for the wild type (Rw) and the other one specific for the mutant (Rm) (Fig. 2). Furthermore, in order to explore how nucleotides involved in substrate binding affect cleavage, we used the wild-type ribozyme to cleave the mutant pre-tRNA and the mutant ribozyme to cleave the wild-type pre-tRNA (Fig. 2). Both ribozymes cleaved the specific pre-tRNA (Sw-Rw and Sm-Rm) at the target site, 3′ to nucleotide 20, yielding two products of 20 and 97 nucleotides. Moreover, the other two combinations were also functional: Rw cleaves Sm and Rm cleaves Sw, both at the expected sites (Fig. 3).

3.2. Temperature dependence of cleavage reactions.

To evaluate the temperature dependence of the four cleavage reactions, a series of time courses were performed using 3:1 molar ratios of S:R at temperatures ranging from 25°C to 60°C (Fig. 4).

At the different temperatures the rates of cleavage varied substantially among the four combinations. The reactions showed the expected temperature dependence considering RNA base pairing possibilities, the cleavage rate increasing with temperature. Cleavage of Sm was generally faster than that of Sw. At 60°C, the wild-type and the mutant pre-tRNA were cleaved with similar efficiency, consistent with melting of the pre-tRNA structure. At temperatures above 40°C, the cleavage of Sw by Rm was faster than its cleavage by Rw. In contrast, at lower temperatures, Sw is cleaved slightly more efficiently by Rw than by Rm. For the other substrate Sm, it

Table 1
Thermodynamic parameters of hammerhead cleavage at 50°C

	Sw-Rw	Sw-Rm	Sm-Rw	Sm-Rm
E_a (kcal/mol)	18	23	19	21
$\Delta G^{\ddagger a}$ (kcal/mol)	20.8	20.6	20.2	19.7
$\Delta H^{\ddagger b}$ (kcal/mol)	17	22	18	20
$\Delta S^{\ddagger c}$ (eu)	−11	5	−6	0

[a]$\Delta G^{\ddagger}$ was calculated from the relationship: $\Delta G^{\ddagger} = -RT\ln(k_{obs}h/k_BT)$, where h is Planck's constant, k_B is Boltzmann's constant, and k_{obs} is the rate constant of cleavage at $T = 323$ K.
[b]$\Delta H^{\ddagger}$ was calculated from the relationship: $\Delta H^{\ddagger} = E_a - RT$.
[c]$\Delta S^{\ddagger}$ was calculated from the relationship: $\Delta G^{\ddagger} = \Delta H^{\ddagger} - T\Delta S^{\ddagger}$; eu: cal/mol per K.

is cleaved better by Rm than by Rw at all the temperatures analyzed.

An Arrhenius plot for each reaction was drawn from the time course data (Fig. 5). The reaction rates showed a linear temperature dependence, no change in the slope of the plot being recognized; the slope of the line gives similar values of activation energies for the four different reactions, around 20 kcal/mol (Table 1), with the highest value being that of Sw-Rm (23 kcal/mol). These values are close to those reported previously for the hammerhead cleavage reactions [11,15,28,29]. The values of the Arrhenius energies (E_a) permit calculation of the thermodynamic activation values, describing the difference in energy levels of reactants and the transition state (Table 1).

3.3. Steady-state kinetics

Cleavage rates were measured during the first few turnovers to help identify which step in the reaction was rate determining and to define conditions appropriate for steady-state measurements (Fig. 6). A lag in the initial turnover could indicate a requirement for a slow conformational change upon substrate binding before the accumulation of an active substrate-ribozyme complex, whereas a rapid initial turnover suggests that product dissociation was the rate determining step. In these reactions, no rate inflections were observed during the approach to steady-state.

Steady-state cleavage velocities were measured for each reaction at several substrate concentrations varying from 0.05 μM to 5 μM, while the concentration of ribozyme remained constant at 0.025 μM.

The reactions follow Michaelis-Menten type kinetics with initial velocities being dependent upon substrate concentration at a constant ribozyme concentration. The results of this type of experiment are shown in an Eadie-Hofstee plot (Fig. 7). The Michaelis-Menten parameters for each type of substrate-ribozyme reaction are listed in Table 2. The k_{cat} values are nearly the same in all 4 cases, while K_m values differ by a factor of 3 among the different type of reactions, the highest K_m being that of Sw-Rw. These results were reproducible in repeated experiments using different preparations of RNAs.

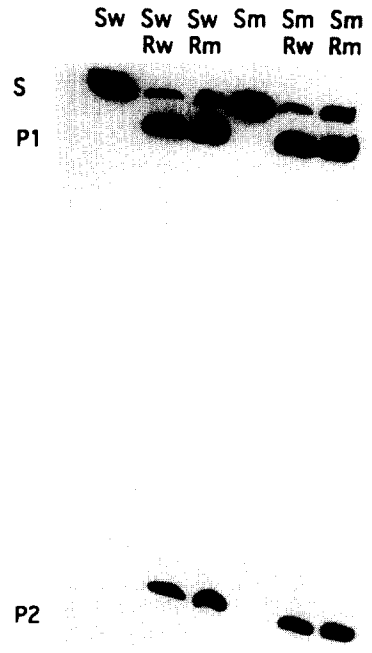

Fig. 3. Denaturing polyacrylamide gel electrophoresis of cleavage reactions. Lanes: 1, Sw without ribozyme; 2, Sw-Rw; 3, Sw-Rm; 4, Sm without ribozyme; 5, Sm-Rw; 6, Sm-Rm. Concentrations of substrates and ribozymes were 0.2 and 0.066 μM, respectively. All reactions where incubated at 50°C for 1 h. S, substrate (117 nucleotides); P1, 3′ cleavage fragment (97 nucleotides); P2, 5′ cleavage fragment (20 nucleotides).

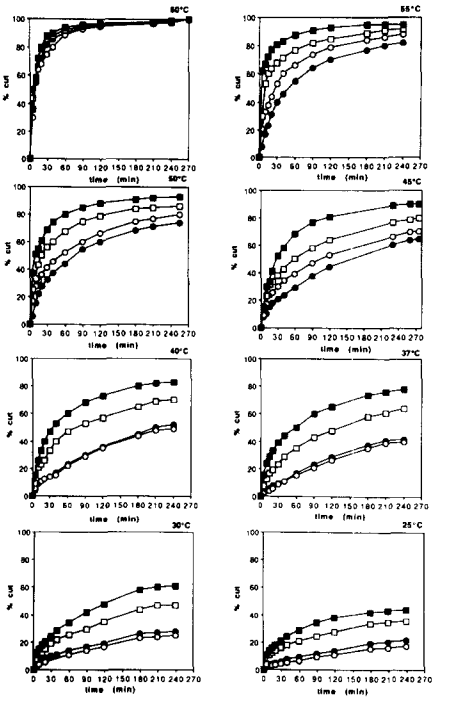

Fig. 4. Time courses of cleavage. The fraction of substrate converted to products at various times is shown for Sw-Rw (●), Sw-Rm (○), Sm-Rw (□), Sm-Rm (■), in reactions containing 0.2 μM substrate and 0.066 μM ribozyme, at temperatures varying between 60°C and 25°C.

Table 2
Michaelis-Menten parameters for ribozyme cleavage

	K_m (μM)	k_{cat} (min^{-1})	k_{cat}/K_m
Sw-Rw	2.9	1.30	0.45
Sw-Rm	2.0	1.20	0.58
Sm-Rw	1.9	1.23	0.65
Sm-Rm	0.9	1.04	1.14

Conditions: 50°C, 0.5–5 μM substrate, 0.025 μM ribozyme, pH 8.0, 10 mM $MgCl_2$.

4. Discussion

Ribozymes provide an interesting alternative to antisense oligonucleotides as antiviral agents and, in general, as inhibitors of the expression of specific genes [16–19]. However, several problems have to be solved in order to target a ribozyme successfully against an RNA sequence. For both exogenous and endogenous delivery, the problem of choosing a suitable target site exists. Since the conformations of RNA molecules are largely stabilized by double-stranded helical regions, it is to be expected that not all potential target sites are equally accessible for ribozyme mediated cleavage. For example, secondary structures, such as a preexisting intramolecular RNA duplex, may preclude access of a ribozyme to its target, or if the ribozyme does hybridize with the target, alternative tertiary structures may form that are more favoured than the hammerhead motif [30].

To examine these problems, here we compare the ribozyme mediated cleavage reactions of pre-$tRNA_3^{leu}$ wild-type and a structurally altered mutant form (Fig. 1); moreover, to analyze the influence of three mismatches in the helix III on cleavage, we use the mutant ribozyme to cleave the wild-type substrate (Sw-Rm) and the wild-type ribozyme to cleave the mutant substrate (Sm-Rw) (Fig. 2).

Comparison of the steady-state kinetics of the four different reactions indicates that the differences in catalytic efficiency are due entirely to differences in K_m values while the k_{cat} values are not affected (Table 2). Thus, the formation of the ribozyme-substrate complex, but not the chemical cleavage step, is affected by these changes. The variation in K_m values among the different substrate-ribozyme reactions may result from the propensity of substrate sequences to form structures that are incompatible with hammerhead assembly. If these structures can equilibrate with cleavable structures during the course of the reaction, high concentrations of substrate will be required to drive complex formation, resulting in a correspondingly high K_m for the reaction. For these reasons, the K_m values of the pre-tRNA substrates are greater than those reported by others [15,20,31–33], who utilized shorter substrates, however, the k_{cat} values are quite similar.

The cleavage reaction Rw-Sw is less efficient than Sm-Rm: it has 3-fold higher K_m and lower rate of cleavage at all temperatures analyzed (Fig. 4). The mutant substrate contains an open D stem, thus the hybridization between substrate and ribozyme is easier.

Furthermore, this mutation can also alter the tertiary structure of mutant pre-tRNA [21], enhancing the cleavage reactions. These results indicate that the structure of the substrate can limit ribozyme efficiency, presumably by hindering the hybridization step [20,34–36].

The analysis of the temperature dependence of cleavage reactions shows that the cleavage efficiency increases with increasing temperature for both Sw and Sm, with Sm being more efficiently cleaved by both ribozymes at all temperatures (Fig. 4). The more efficient cleavage at higher temperatures could result from the shifting of the equilibrium between the substrate structures incompatible with hammerhead cleavage and the active conformations, as well as affecting the dissociation and reannealing of substrate and ribozyme molecules.

An Arrhenius plot for each reaction was drawn from the temperature dependence of the cleavage (Fig. 5). The Arrhenius plot may be non-linear if different steps become the rate-limiting step at different temperatures. Since no change in the slope of the plots was recognized, the rate-determining step seems to be the same for all temperatures [29]. From the Arrhenius plot, the activation energy, enthalpy and entropy changes required to reach the transition state were calculated (Table 1). The enthalpy of activation ($\Delta H^{\ddagger}$) for the Sw-Rw reaction (17 kcal/mol) is lower than that of the Sm-Rm reaction (20 kcal/mol), but there is no entropy change ($\Delta S^{\ddagger}$) for

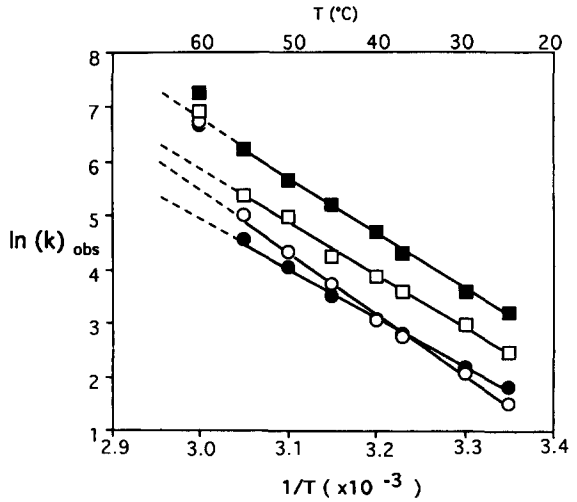

Fig. 5. Arrhenius plots of the cleavage reactions. The logarithm of the second-order rate constant of cleavage (K mM^{-1} min^{-1}), is plotted versus the temperature ($1/T \times 10^{-3}$), for Sw-Rw (●), Sw-Rm (○), Sm-Rw (□), Sm-Rm (■).

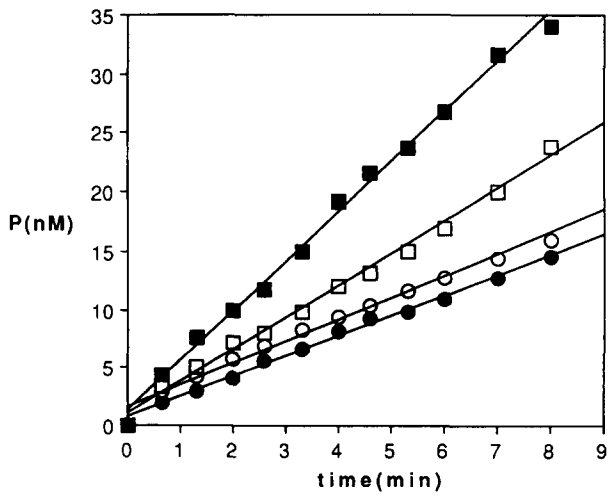

Fig. 6. Cleavage kinetics during the approach to steady-state. The concentration of products (P) is plotted versus time for Sw-Rw (●), Sw-Rm (○), Sm-Rw (□), Sm-Rm (■), in reactions with 0.2 μM substrate and 0.066 μM ribozyme, incubated at 50°C.

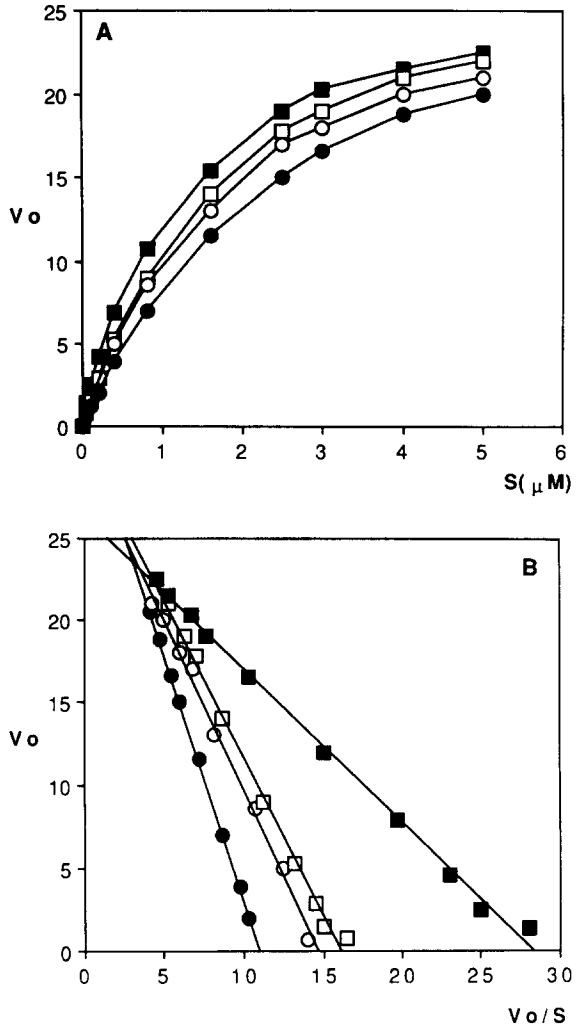

Fig. 7. Steady-state kinetics of ribozyme cleavage reactions. (A) The steady-state rate of cleavage (V_o, nM min^{-1}) is plotted versus substrate (S) concentrations for Sw-Rw (●), Sw-Rm (○), Sm-Rw (□), Sm-Rm (■). Ribozyme concentration was 0.025 μM; reactions were performed at 50°C. (B) Eadie-Hofstee plots of the data.

the Sm-Rm reaction while the $\Delta S^{\ddagger}$ value for the Sw-Rw reactions (−11 eu) is considerably more unfavourable. The reaction Sw-Rm has the largest value of enthalpy of activation (22 kcal/mol), but this value is compensated by a positive value of $\Delta S^{\ddagger}$ (5 eu).

The overall ribozyme efficiency is likely to depend on both the length and base composition of the sequence that hybridizes with the target sequence in the substrate. Optimal efficiency will be provided with any complementary sequence long enough to allow formation of a sufficiently stable enzyme/substrate complex, but short enough to allow a high rate of product release. To estimate the importance of these two parameters, we have used the mutant ribozyme to cleave the wild-type substrate (Sw-Rm) and the wild-type ribozyme to cleave the mutant substrate (Sm-Rw) (Fig. 2). The presence of three mismatches in helix III of the Sw-Rm combination increases ribozyme efficiency compared with the Sw-Rw reaction, at temperatures above 40°C, probably caused by promoting ribozyme turnover. Instead, at lower temperatures, the Sw-Rm reaction is less efficient than Sw-Rw; in this case the greater affinity between ribozyme and substrate could enhance the cleavage reaction. In contrast, for the mutant pre-tRNA, the presence of three mismatches in the helix III (Sm-Rw), makes the cleavage reaction less efficient compared with the reaction between Sm-Rm at all the temperatures analyzed. One can postulate the absence of mismatches increase the affinity between ribozyme and substrate and since AU base-pairs are less stable than CG base-pairs which are present in the Sw-Rw, this combination would allow greater ribozyme turnover.

In summary, these studies show that with a large RNA target, the substrate-ribozyme binding seems to be the crucial step, the difference in accessibility at the same site of substrate with different structure and the importance of length and nucleotide sequence of the ribozyme-substrate hybridizing region.

Acknowledgements: We thank Kelly Williams, Thomas Wagner and Andrea Stoler for helpful discussions and critical reading of this manuscript. This work was supported by Progetto Finalizzato (CNR) Ingegneria Genetica, Human Frontiers Science Program Organization (HFSPO), Progetto Strategico (CNR) 'Nucleotidi antisenso come strumento di nuove strategie terapeutiche' and by Progetto Finalizzato (CNR) Biotecnologie e Biostrumentazione).

References

[1] Noller, H.F., Hoffarth,V. and Zimniak, L. (1992) Science 256, 1416–1419.
[2] Piccirilli, J.A., McConnell, T.S., Zaug, A.J., Noller, H.F. and Cech, T.R. (1992) Science 256, 1420–1424.
[3] Cech, T.R. (1990) Angew. Chem. Int. Ed. Engl. 29, 759–768.
[4] Altman, S. (1989) Adv. Enzymol. 62, 1–36.
[5] Symons, R.H. (1989) Trends Biochem. Sci. 14, 445–450.
[6] Keese, P. and Symons, R.H. (1987) in: Viroids and Viroid-like Pathogens (Semancik, J.S. ed.) pp. 1–47, CRC Press, Boca Raton, FL.
[7] Pley, H.W., Flaherty, K.M. and McKay, D.B. (1994) Nature 372, 68–74.
[8] Scott, W.G., Finch, J.T. and Klug, A. (1995) Cell 81, 991–1002.
[9] Buzayan, J.M., Gerolach, W.L. and Breuning, G. (1986) Procl. Natl. Acad. Sci. USA 83, 8859–8862.
[10] Forster, A. and Symons, R.H. (1987) Cell 50, 9–16.
[11] Uhlenbeck, O.C. (1987) Nature 328, 596–600.
[12] Ruffner, D.E., Dahm, S.C. and Uhlenbeck, O.C. (1989) Gene 82, 31–41.
[13] Koizumi, M., Iwai, S. and Ohtsuka, E. (1988) FEBS Lett. 228, 228–230.
[14] Haseloff, J. and Gerlach, W.L. (1988) Nature 334, 585–591.
[15] Jeffries, A.C. and Symons, R.H. (1989) Nucleic Acids Res. 17, 1371–1377.
[16] Sarver, N., Cantin, E.M., Chang, P.S., Zaia, J.A., Ladne, P.A., Stephens, D.A. and Rossi, J.J. (1990) Science 247, 1222–1225.
[17] Cantor, G.H., McElwain, T.F., Birkebak, T.A. and Palmer, G.H. (1993) Proc. Natl. Acad. Sci. USA 90, 10932–10936.
[18] Ohkawa, I., Yuyama, N., Takebe, Y., Nishikawa, S. and Taira, K. (1993) Proc. Natl. Acad. Sci. USA 90, 11302–11306.
[19] Altman, S. (1993) Proc. Natl. Acad. Sci. USA 90, 10898–10900.
[20] Fedor, M.J. and Uhlenbeck O.C. (1990) Proc. Natl. Acad. Sci. USA 87, 1668–1672.
[21] Baldi, M.I., Mattoccia, E. and Tocchini-Valentini, G.P. (1983) Cell 35, 109–115.
[22] Reyes, V.M. and Abelson, J. (1987) Anal. Biochem. 166, 90–95.
[23] Melton, D.A., Krieg, P.A., Rebagliati, M.R., Maniatis, T., Zinn, K. and Green, M.R. (1984) Nucleic Acids Res. 12, 7035–7039.
[24] Milligan, J.F., Groebe, D.R., Witherell, G.W. and Uhlenbeck, O.C. (1987) Nucleic Acids Res. 15, 8783–8798.
[25] Groebe, D.R. and Uhlenbeck O.C. (1988) Nucleic Acids Res. 16, 11725–11735.
[26] Eadie, G.S. (1942) J. Biol. Chem. 146, 85–93.
[27] Hofstee, B.H.J. (1952) J. Biol. Chem. 199, 357–364.
[28] Hertel, K.J. and Uhlenbeck, O.C. (1995) Biochemistry 34, 1744–1749.

[29] Takagi, Y. and Taira, K. (1995) FEBS Lett. 361, 273–276.
[30] Bertrand, E., Grange, T. and Pictet, R. (1992) in: Gene Regulation: Biology of Antisense RNA and DNA (Erickson, R.P. and Izant, J.G. eds.) pp. 71–78, Raven, New York.
[31] Hertel, K.J., Herschlag, D. and Uhlenbeck, O.C. (1994) Biochemistry 33, 3374–3385.
[32] Fedor, M.J. and Uhlenbeck, O.C. (1992) Biochemistry 31, 12042–12054.
[33] Long, D.M. and Uhlenbeck, O.C. (1994) Proc. Natl. Acad. Sci. USA 91, 6977–6981.
[34] Heidenreich, O. and Eckstein, F. (1992) J. Biol. Chem. 267, 1904–1909.
[35] Bertrand, E., Pictet, R. and Grange T. (1994) Nucleic Acids Res. 22, 293–300.
[36] Ellis, J. and Rogers, J. (1993) Nucleic Acids Res. 22, 5171–5178.